**Immunity, Volume *46***

## Supplemental Information

# A Relay Pathway between Arginine and Tryptophan Metabolism Confers Immunosuppressive Properties on Dendritic Cells

**Giada Mondanelli, Roberta Bianchi, Maria Teresa Pallotta, Ciriana Orabona, Elisa Albini, Alberta Iacono, Maria Laura Belladonna, Carmine Vacca, Francesca Fallarino, Antonio Macchiarulo, Stefano Ugel, Vincenzo Bronte, Federica Gevi, Lello Zolla, Auke Verhaar, Maikel Peppelenbosch, Emilia Maria Cristina Mazza, Silvio Bicciato, Yasmina Laouar, Laura Santambrogio, Paolo Puccetti, Claudia Volpi, and Ursula Grohmann**

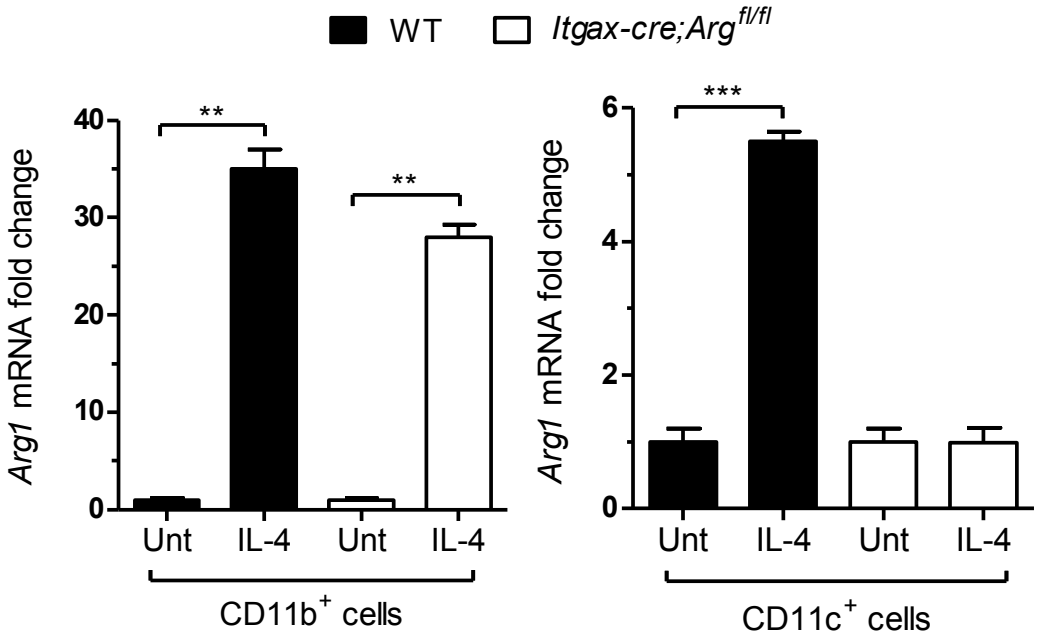


**Figure S1. CD11b$^+$ but not CD11c$^+$ cells from *Itgax-cre;Arg1$^{fl/fl}$* upregulate *Arg1* expression in response to IL-4 (related to Figure 2).** Real-time PCR analysis of *Arg1* transcripts in CD11b$^+$ and CD11c$^+$ cells purified from the spleen of wild-type (WT) or *Itgax-cre;Arg1$^{fl/fl}$* mice and stimulated for 3 hr with IL-4. Data were normalized to the expression of *Gapdh* (encoding glyceraldehyde phosphate dehydrogenase) and are presented relative to results in untreated cells. One experiment representative of three,

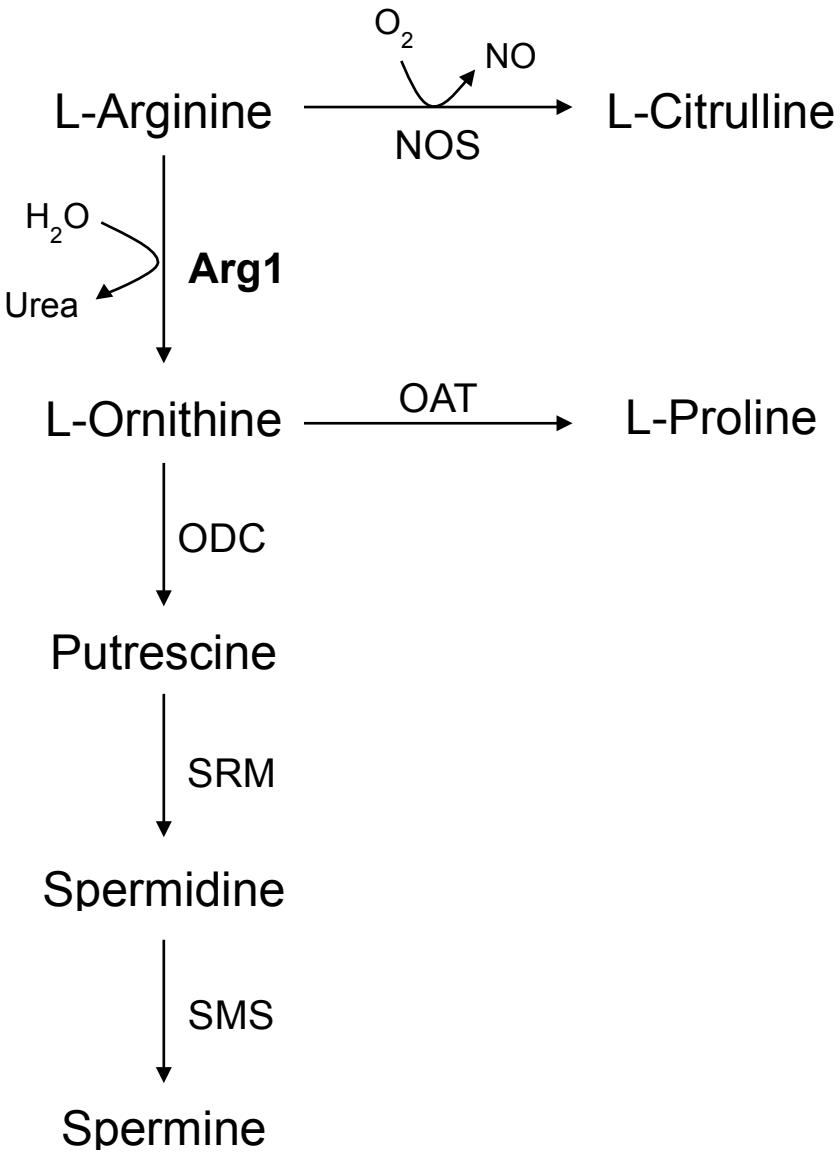


**Figure S2. Scheme of the Arg1 Pathway (related to Figure 5).** The reaction catalyzed by nitric oxide synthases (NOS) is also shown. OAT, ornithine aminotransferase. ODC, ornithine decarboxylase. SRM, spermidine synthase. SMS, spermine synthase.

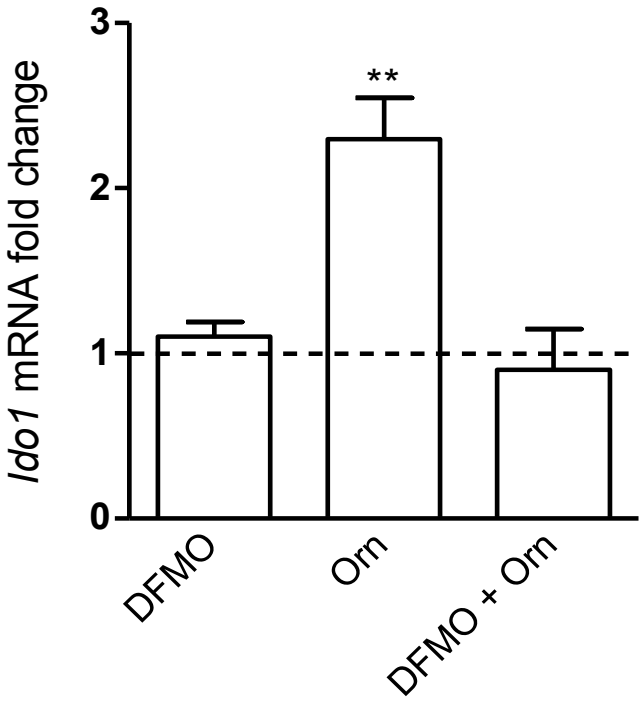


**Figure S3. Orn Upregulates *IDO1* Expression in Human DCs via ODC Catalytic Activity (related to Figure 5).** DCs ($5 \times 10^5$), obtained as described in Experimental Procedures, were exposed to 1 mM DFMO or medium alone for 1 hr prior to incubation with Orn at 100 μM or medium for 24 hr. Expression of *IDO1* transcripts was evaluated by Real-Time PCR, normalized to the expression of *ACTB* (i.e., the human β-actin encoding gene), and presented relative to values in untreated cells (fold change = 1; dotted line). **, $p < 0.01$ (unpaired Student's *t* test; DCs treated with DFMO, Orn, or a combination of both *vs.* untreated samples). One experiment representative of three.

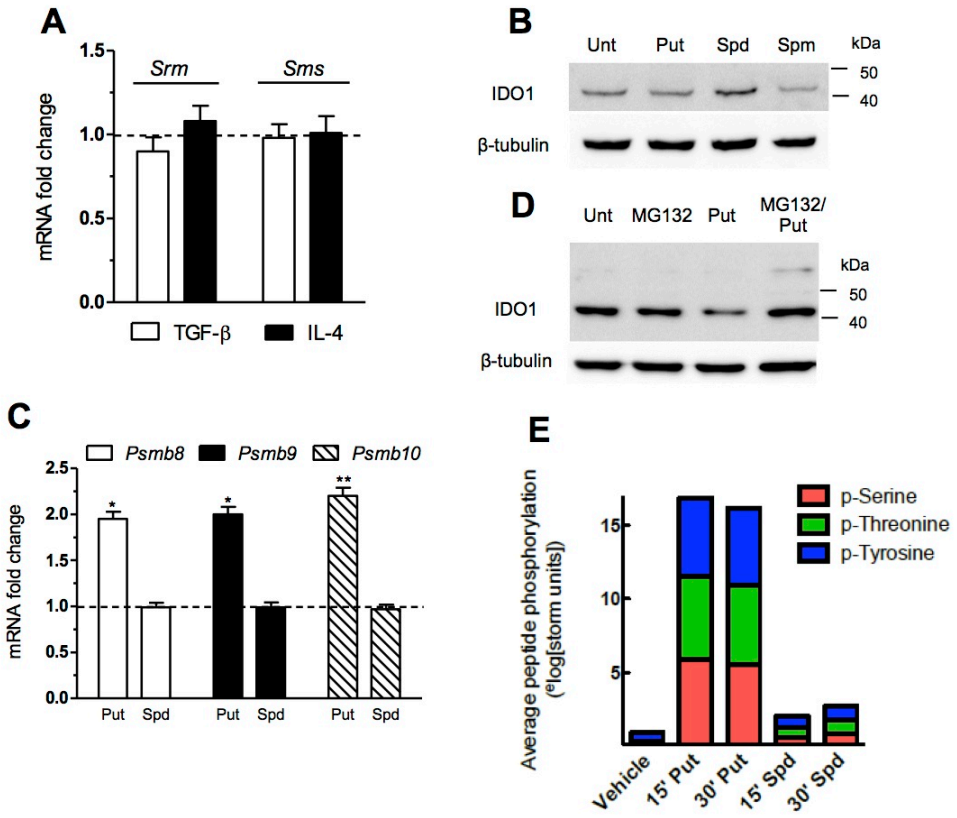


**Figure S4. Effect of Polyamines on IDO1 Protein Expression and Activation of Kinases in DCs (related to Figure 6).**

(A) Real-time PCR analysis of *Srm* (coding for spermidine synthase) and *Sms* (spermine synthase) gene expression in DCs stimulated with TGF-β or IL-4 for 18 hr, normalized to the expression of *Gapdh* (encoding glyceraldehyde phosphate dehydrogenase) and presented relative to results in untreated cells (dotted line, one fold).

(B) Splenic DCs from WT mice were incubated with 20 μM putrescine (Put), spermidine (Spd), or spermine (Spm) and, after 24 hr, cell lysates were examined for IDO1 expression by means of a specific anti-mouse IDO1 antibody. β-tubulin expression was used as a loading control.

(C) Real-time PCR analysis of *Psmb8, Psmb9, and Psmb10* (coding for β5i, β1i, and β2i immunoproteasome subunits, respectively) gene expression in DCs incubated with putrescine or spermidine for 18 hr, normalized as in (A).

(D) Splenic DCs from WT mice were incubated with 5 μg/ml cycloheximide (an inhibitor of protein synthesis) for 30 min prior to addition of 10 μM MG132 (a proteasome inhibitor), 20 μM putrescine (Put), or a combination of both. Control cells (Unt) were treated with cycloheximide and then incubated with medium alone. After 3 hr, cell lysates were examined for IDO1 expression by means of a specific anti-mouse IDO1 antibody. β-tubulin expression was used as a loading control.

(E) Average of serine, threonine, and tyrosine phosphorylation of Chip peptides in DCs incubated with putrescine (Put) or spermidine (Spd) for 15 or 30 min. Untreated cells (vehicle) were used control. One experiment representative of two (D and E) or three (A-C) is shown.

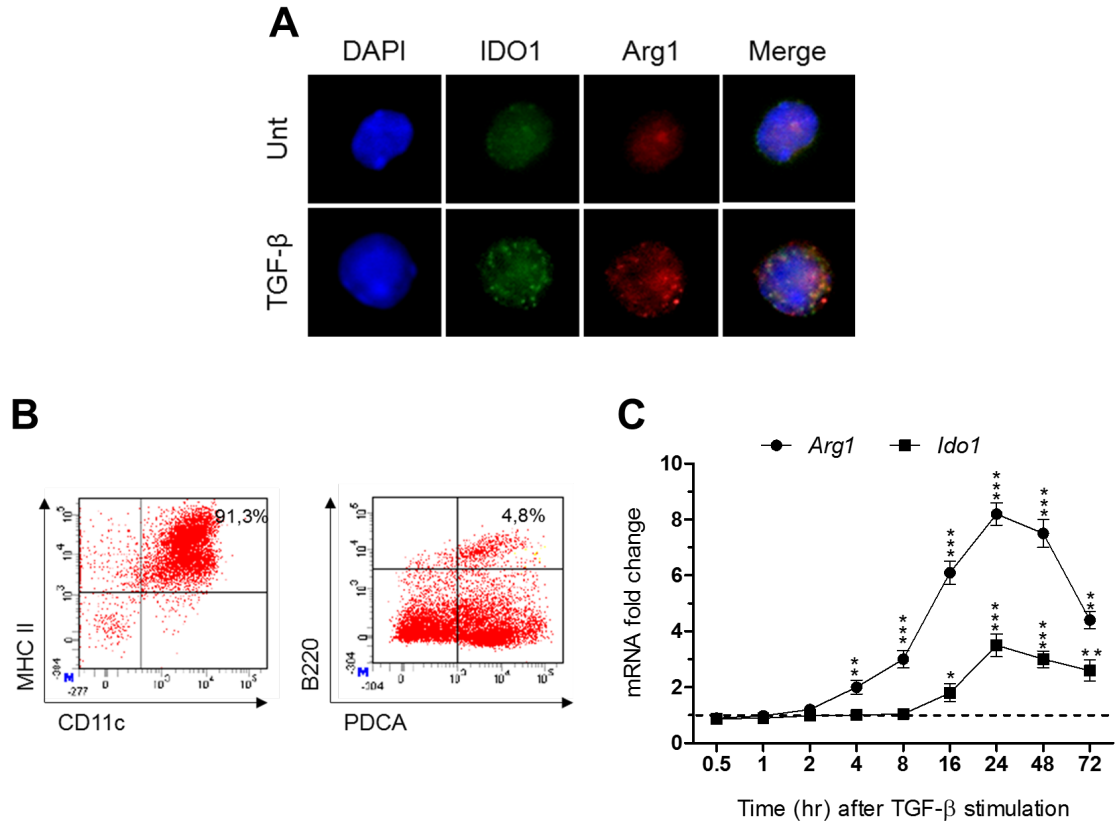


**Figure S5. Co-expression of Arg1 and IDO1 in DCs and upregulation of both *Arg1* and *Ido1* transcripts by TGF-β in plasmacytoid DCs (related to Figure 7 and Experimental Procedures).**

(A) Immunofluorescence analysis of DCs, incubated with medium alone (Unt) or stimulated with TGF-β for 24 hr and stained with anti-Arg1 (red) and anti-IDO1 (green) antibodies. Nuclei were stained with DAPI (blue).

(B) Cytofluorimetric analysis of DCs purified from the mouse spleen. Cells were stained with anti-CD11c and –MHC II (to evaluate cDC purity) or anti-B220 and –PDCA (to evaluate the contamination of pDCs) antibodies. Numbers show percentages of positive cells in the indicate gate. The fact that PDCA alone but not in combination with B220 was highly expressed in the DC population may derive from nonspecific effects of cell manipulation *in vitro*, as previously reported (Blasius et al., 2006).

(C) Kinetic analysis of *Arg1* and *Ido1* transcripts in purified pDCs from WT mice after incubation with TGF-β for different times (indicated). Data are normalized to the expression of *Gapdh* and presented relative to results in untreated cells (dotted line, one fold). In (A-C), one representative experiment out of four (A and B) or three (C) is shown.

**Table S1. Modulation of Src-like Kinase Activity Following Stimulation with Putrescine or Spermidine (related to Fig. 6)**

Kinase activity in vehicle control cultures and those stimulated with putrescine or spermidine towards Src-like kinase signal-transduction-relevant undecapeptides. Cells were lysed and analysed by *in vitro* kinase assays as described in the Experimental Procedures section (see also Figure S4B). Results (in artificial phosphoimager units) represent the average value and standard deviation obtained from three technical replicas (three separate reactions carried out in parallel). Values are STORM phosphoimager units (24 hr exposure).

| Peptide used for kinase reaction | Phosphorylation site in protein | Upstream kinase | Vehicle | 15'putrescine | 30'putrescine | 15'spermidine | 30'spermidine |
|---|---|---|---|---|---|---|---|
| PCTTIYVAATE | $SLAM_{Tyr307}$ | Fyn | $1.0 \pm 0.0 \cdot 10^{0}$ | 0.0 | $3.2 \pm 0.0 \cdot 10^{1}$ | 0.0 | $1.0 \pm 0.0 \cdot 10^{0}$ |
| EELAEYAEIRV | $SIGLEC4A_{Tyr620}$ | Fyn | $2.0 \pm 0.0 \cdot 10^{0}$ | $3.0 \pm 0.0 \cdot 10^{1}$ | 0.0 | $1.0 \pm 0.0 \cdot 10^{0}$ | 0.0 |
| SLESLYSACSM | $Grb10_{Tyr61}$ | Fyn | $2.0 \pm 1.0 \cdot 10^{0}$ | $9.9 \pm 0.0 \cdot 10^{1}$ | 0.0 | 0.0 | $2.0 \pm 0.0 \cdot 10^{0}$ |
| DDQEVYDDVAE | $FYB_{Tyr595}$ | Fyn | $1.7 \pm 0.6 \cdot 10^{0}$ | $1.3 \pm 0.7 \cdot 10^{2}$ | $1.5 \pm 0.2 \cdot 10^{2}$ | $3.0 \pm 0.0 \cdot 10^{0}$ | $2.0 \pm 0.0 \cdot 10^{0}$ |
| KAGNLYDISED | $NR2B_{Tyr1259}$ | Fyn | 0.0 | $1.5 \pm 0.0 \cdot 10^{2}$ | $3.3 \pm 0.0 \cdot 10^{1}$ | $1.0 \pm 0.0 \cdot 10^{0}$ | $1.0 \pm 0.0 \cdot 10^{0}$ |
| **VNLINYQDDAE** | **$CTNNB1_{Tyr142}$** | **Fyn** | **0.0** | **0.0** | **0.0** | **0.0** | **$8.0 \pm 0.0 \cdot 10^{0}$** |
| DVLKFYDSNTV | $PAK2_{Tyr130}$ | Hck | $2.3 \pm 0.6 \cdot 10^{0}$ | $3.0 \pm 0.0 \cdot 10^{2}$ | $2.6 \pm 0.4 \cdot 10^{2}$ | $4.0 \pm 0.0 \cdot 10^{0}$ | $3.0 \pm 1.4 \cdot 10^{0}$ |
| IPSVPYAPFAA | $GNRF2_{Tyr522}$ | Hck | $2.0 \pm 0.0 \cdot 10^{0}$ | $1.2 \pm 0.0 \cdot 10^{2}$ | $1.8 \pm 0.2 \cdot 10^{2}$ | $2.0 \pm 0.0 \cdot 10^{0}$ | 0.0 |
| DEGDEIYEDLMR | $Vav_{Tyr174}$ | Lck | $1.0 \pm 0.0 \cdot 10^{0}$ | $7.8 \pm 0.5 \cdot 10^{1}$ | $8.2. \pm 4.7 \cdot 10^{1}$ | 0.0 | $1.0 \pm 0.0 \cdot 10^{0}$ |
| FDDPSYVNVQN | $Shc_{Tyr427}$ | Lck | $4.3 \pm 1.5 \cdot 10^{0}$ | $3.2 \pm 1.2 \cdot 10^{2}$ | $7.9 \pm 0.0 \cdot 10^{1}$ | $2.6 \pm 0.6 \cdot 10^{0}$ | $3.5 \pm 0.7 \cdot 10^{0}$ |
| GGDDIYEDIIK | $Vav2_{Tyr172}$ | Lck | $2.0 \pm 1.4 \cdot 10^{0}$ | $3.3 \pm 3.8 \cdot 10^{2}$ | $1.3 \pm 0.7 \cdot 10^{2}$ | $2.3 \pm 0.6 \cdot 10^{0}$ | $2.0 \pm 0.0 \cdot 10^{0}$ |
| TTVELYSLAER | $PKC\theta_{Tyr90}$ | Lck | 0.0 | 0.0 | 0.0 | $2.0 \pm 0.0 \cdot 10^{0}$ | $1.0 \pm 0.0 \cdot 10^{0}$ |
| IKEDVYLSHDH | $PTK6_{Tyr342}$ | Lck | 0.0 | $2.8 \pm 1.2 \cdot 10^{2}$ | $2.4 \pm 0.4 \cdot 10^{2}$ | $3.5 \pm 0.7 \cdot 10^{0}$ | $3.0 \pm 0.7 \cdot 10^{0}$ |
| LNEEWYVSYIT | $SKP76_{Tyr423}$ | Lck | $4.3 \pm 1.0 \cdot 10^{0}$ | $3.1 \pm 0.2 \cdot 10^{2}$ | $3.6 \pm 0.4 \cdot 10^{2}$ | $4.0 \pm 1.0 \cdot 10^{0}$ | $3.7 \pm 0.6 \cdot 10^{0}$ |
| SRLSAYPALEG | $CD5_{Tyr487}$ | Lck | $1.5 \pm 0.7 \cdot 10^{0}$ | $1.6 \pm 0.4 \cdot 10^{2}$ | $1.5 \pm 0.6 \cdot 10^{2}$ | $1.0 \pm 0.0 \cdot 10^{0}$ | $2.3 \pm 2.3 \cdot 10^{0}$ |
| ADDSYYTARSA | $ZAP70_{Tyr493}$ | Lck | $3.0 \pm 0.0 \cdot 10^{0}$ | $1.5 \pm 0.0 \cdot 10^{2}$ | $2.1 \pm 0.5 \cdot 10^{2}$ | $3.5 \pm 2.1 \cdot 10^{0}$ | $1.7 \pm 0.6 \cdot 10^{0}$ |
| AEKPFYVNVEF | $BCR_{Tyr177}$ | Lyn | 0.0 | $1.6 \pm 0.7 \cdot 10^{2}$ | $1.6 \pm 0.9 \cdot 10^{2}$ | $1.6 \pm 0.6 \cdot 10^{0}$ | $2.0 \pm 0.0 \cdot 10^{0}$ |
| VLDDEYVSSFG | $TXK_{Tyr420}$ | Lyn | $1.0 \pm 0.0 \cdot 10^{0}$ | $1.9 \pm 0.0 \cdot 10^{2}$ | $1.4 \pm 0.0 \cdot 10^{2}$ | 0.0 | $1.0 \pm 0.0 \cdot 10^{0}$ |
| FNNPAYYVLEG | $IPPL1_{Tyr986}$ | Lyn | 0.0 | 0.0 | $5.3 \pm 0.0 \cdot 10^{1}$ | $1.0 \pm 0.0 \cdot 10^{0}$ | $2.0 \pm 1.0 \cdot 10^{0}$ |
| LGSQSYEDMRG | $CD19_{Tyr531}$ | Lyn | $1.5 \pm 0.7 \cdot 10^{0}$ | $1.8 \pm 1.2 \cdot 10^{2}$ | $1.1 \pm 0.0 \cdot 10^{2}$ | $2.0 \pm 0.0 \cdot 10^{0}$ | $1.5 \pm 0.7 \cdot 10^{0}$ |
| ETNNDYETADG | $CD32_{Tyr279}$ | Lyn | 0.0 | $1.1 \pm 0.5 \cdot 10^{2}$ | 0.0 | $1.5 \pm 0.7 \cdot 10^{0}$ | $1.0 \pm 0.0 \cdot 10^{0}$ |
| RRCKHYVELLV | $VRLC2_{Tyr253}$ | Lyn | $3.7 \pm 0.6 \cdot 10^{0}$ | $1.2 \pm 0.1 \cdot 10^{2}$ | $1.7 \pm 0.1 \cdot 10^{2}$ | $3.0 \pm 0.7 \cdot 10^{0}$ | $1.7 \pm 0.6 \cdot 10^{0}$ |
| FSGGLYGGLPP | $NIPP1_{Tyr264}$ | Lyn | $2.0 \pm 0.0 \cdot 10^{0}$ | $7.6 \pm 3.2 \cdot 10^{1}$ | $1.1 \pm 0.0 \cdot 10^{2}$ | $1.5 \pm 0.7 \cdot 10^{0}$ | $1.0 \pm 0.0 \cdot 10^{0}$ |

| | | | | | | | |
|---|---|---|---|---|---|---|---|
| MRGILYAAPQL | $CD19_{Tyr409}$ | Lyn | $1.0 \pm 0.0 \cdot 10^{0}$ | $1.1 \pm 0.0 \cdot 10^{2}$ | $0.5 \pm 0.0 \cdot 10^{2}$ | 0.0 | $2.0 \pm 0.0 \cdot 10^{0}$ |
| **FFVIEYVNGGD** | **$PKC\iota_{Tyr325}$** | **Src** | **0.0** | **0.0** | **$5.8 \pm 0.0 \cdot 10^{1}$** | **0.0** | **$4.3 \pm 0.0 \cdot 10^{1}$** |
| TIPPKYRELLA | $Calpastatin_{Tyr205}$ | Src | $2.0 \pm 0.0 \cdot 10^{0}$ | $1.6 \pm 0.0 \cdot 10^{2}$ | $6.2 \pm 4.2 \cdot 10^{1}$ | $1.0 \pm 0.0 \cdot 10^{0}$ | $2.0. \pm 1.0 \cdot 10^{0}$ |
| FDAHIYEGRVI | $PKC\delta_{Ty64}$ | Src | $2.3 \pm 0.6 \cdot 10^{0}$ | $2.2 \pm 0.7 \cdot 10^{2}$ | $1.8 \pm 0.9 \cdot 10^{2}$ | $2.7 \pm 0.6 \cdot 10^{0}$ | $3.3. \pm 0.6 \cdot 10^{0}$ |
| AEDSTYDEYEN | $Cortactin_{Ty486}$ | Src | 0.0 | $1.3 \pm 0.5 \cdot 10^{2}$ | $9.1 \pm 2.7 \cdot 10^{1}$ | 0.0 | $1.0 \pm 0.0 \cdot 10^{0}$ |
| IDAFSDYANFK | $RPTP\alpha_{Ty798}$ | Src | $1.5 \pm 0.7 \cdot 10^{0}$ | $1.3 \pm 0.5 \cdot 10^{2}$ | $1.1 \pm 0.7 \cdot 10^{2}$ | $2.0 \pm 0.0 \cdot 10^{0}$ | 0.0 |
| NGRPDYIIVTQ | $ArylhydrocarbonR_{Ty378}$ | Src | 0.0 | $7.5 \pm 0.0 \cdot 10^{1}$ | 0.0 | 0.0 | $1.0 \pm 0.0 \cdot 10^{0}$ |
| CGSQKYAYFNG | $Conexin43_{Tyr265}$ | Src | 0.0 | $2.0 \pm 1.7 \cdot 10^{2}$ | $1.9 \pm 0.2 \cdot 10^{2}$ | $2.3 \pm 1.5 \cdot 10^{0}$ | $2.0 \pm 1.4 \cdot 10^{0}$ |
| AEEKEYHAEGG | $EGFR_{Tyr869}$ | Src | $1.2 \pm 1.3 \cdot 10^{1}$ | $2.0 \pm 0.0 \cdot 10^{2}$ | $1.0 \pm 0.0 \cdot 10^{2}$ | $2.0 \pm 0.0 \cdot 10^{0}$ | 0.0 |
| PATDLYQVPPG | $p130CAS_{Tyr165}$ | Src | $2.3 \pm 0.6 \cdot 10^{0}$ | $5.2 \pm 1.9 \cdot 10^{2}$ | $3.3 \pm 1.3 \cdot 10^{2}$ | $3.0 \pm 1.0 \cdot 10^{0}$ | $2.5 \pm 0.7 \cdot 10^{0}$ |
| GIWKASFTTFT | $Caveolin1_{Tyr14}$ | Src | $1.0 \pm 0.0 \cdot 10^{0}$ | $6.1 \pm 3.9 \cdot 10^{2}$ | $4.0 \pm 2.3 \cdot 10^{2}$ | $4.0 \pm 1.4 \cdot 10^{0}$ | $3.0 \pm 0.0 \cdot 10^{0}$ |
| GWMVHYTSKDT | $PKC\mu_{Tyr432}$ | Src | $2.0 \pm 1.4 \cdot 10^{0}$ | $1.8 \pm 0.0 \cdot 10^{2}$ | 0.0 | $2.0 \pm 0.0 \cdot 10^{0}$ | 0.0 |
| IEDNEYTARQG | $Src_{Tyr419}$ | Src | 0.0 | $1.1 \pm 0.5 \cdot 10^{2}$ | $2.4 \pm 0.0 \cdot 10^{2}$ | $1.0 \pm 0.0 \cdot 10^{0}$ | 0.0 |
| LEDNDYGRAVD | $PKB_{Tyr326}$ | Src | 0.0 | $3.4 \pm 0.0 \cdot 10^{2}$ | $1.5 \pm 1.0 \cdot 10^{2}$ | $1.7 \pm 0.6 \cdot 10^{0}$ | $2.5 \pm 0.7 \cdot 10^{0}$ |
| DEELHYASLNF | $CD33_{Tyr340}$ | Src | $2.7 \pm 1.5 \cdot 10^{0}$ | $2.3 \pm 0.3 \cdot 10^{2}$ | $2.1 \pm 0.3 \cdot 10^{2}$ | $2.0 \pm 0.0 \cdot 10^{0}$ | $2.0 \pm 1.0 \cdot 10^{0}$ |
| PRSTHTAYIK | $ADAM12_{Tyr907}$ | Src | $1.0 \pm 0.0 \cdot 10^{0}$ | $2.5 \pm 0.0 \cdot 10^{2}$ | $0.5 \pm 0.0 \cdot 10^{2}$ | $1.0 \pm 0.0 \cdot 10^{0}$ | $1.7 \pm 1.0 \cdot 10^{0}$ |
| DDEDCYGNYDN | $PDK1_{Tyr373}$ | Src | $2.0 \pm 0.0 \cdot 10^{0}$ | $1.8 \pm 0.0 \cdot 10^{2}$ | $2.5 \pm 1.0 \cdot 10^{2}$ | $4.0 \pm 1.0 \cdot 10^{0}$ | $1.0 \pm 0.0 \cdot 10^{0}$ |
| ITEEDYQALRT | $Clathrin1_{Tyr1477}$ | Src | $1.0 \pm 0.0 \cdot 10^{0}$ | $1.3 \pm 0.0 \cdot 10^{2}$ | $2.1 \pm 0.0 \cdot 10^{2}$ | 0.0 | $1.5 \pm 0.7 \cdot 10^{0}$ |
| TTSQLYDAVPI | $PDK1_{Tyr9}$ | Src | 0.0 | 0.0 | 0.0 | 0.0 | 0.0 |
| PKDEVYSKYYT | $STAT5B_{Tyr679}$ | Src | 0.0 | $1.5 \pm 0.0 \cdot 10^{2}$ | $6.3 \pm 0.6 \cdot 10^{1}$ | 0.0 | 0.0 |
| FTNPVYATLYM | $LDLRRP1_{Tyr4507}$ | Src | $2.0 \pm 0.0 \cdot 10^{0}$ | $1.4 \pm 0.8 \cdot 10^{2}$ | $1.2 \pm 0.4 \cdot 10^{2}$ | $2.0 \pm 1.0 \cdot 10^{0}$ | $3.0 \pm 0.0 \cdot 10^{0}$ |
| DIDGQYAMTRA | $\beta\text{-}Catenin_{Tyr86}$ | Src | 0.0 | $2.7 \pm 0.0 \cdot 10^{2}$ | $2.8 \pm 0.0 \cdot 10^{2}$ | $2.5 \pm 0.7 \cdot 10^{0}$ | $2.0 \pm 1.4 \cdot 10^{0}$ |
| VLDDQYVSSVG | $BMX_{Tyr566}$ | Src | 0.0 | $1.2 \pm 0.7 \cdot 10^{2}$ | 0.0 | $2.0 \pm 0.0 \cdot 10^{0}$ | $3.0 \pm 1.4 \cdot 10^{0}$ |
| EQRNVYKDYRQ | $Dynamin1_{Tyr597}$ | Src | 0.0 | $4.1 \pm 0.2 \cdot 10^{2}$ | $2.7 \pm 0.8 \cdot 10^{2}$ | $2.3 \pm 0.6 \cdot 10^{0}$ | $3.0 \pm 0.0 \cdot 10^{0}$ |

Peptides in bold are those mentioned in the main text.

**Table S2. Sequence of Primers Used in Real-Time Experiments (related to Experimental Procedures)**

| Gene | Forward primer (5'- 3') | Reverse primer (5'- 3') |
|---|---|---|
| *Ido1* | CGATGTTCGAAAGGTGCTGC | GCAGGAGAAGCTGCGATTTC |
| *Arg1* | CAGAAGAATGGAAGAGTCAG | CAGATATGCAGGGAGTCACC |
| *Ptpn6* | CAGCTGCTAGGTCCAGATGAGA | CAGCTCAGGTACTGGTAGTGC |
| *Tgfb1* | CACAGAGAAGAACTGCTGTG | AGGAGCGCACAATCATGTTG |
| *Gapdh* | CTGCCCAGAACATCATCCCT | ACTTGGCAGGTTTCTCCAGG |
| *IDO1* | TCACAGACCACAAGTCACAG | GCAAGACCTTACGGACATCT |
| *ACTB* | TCAGGGTGAGGATGCCTCTC | CTCGTCGTCGACAACGGCT |

**Table S3. Complete List of Arrays Used in This Study (related to Fig. 5)**

Gene expression data of DCs, obtained using Mouse Gene 1.0 ST and Mouse Genome 430 2.0 arrays, were downloaded from Gene Expression Omnibus (http://www.ncbi.nlm.nih.gov/geo) and ArrayExpress (https://www.ebi.ac.uk/arrayexpress/).

**Table S4. Peptide array raw data (related to Figure 6 and Figure S4)**

For peptide array analysis, we employed the Pepchip kinomics array, featuring 960 different human-only kinase substrate peptides in addition to 70 positive and negative controls, each spotted in triplicate. The chips were exposed to a phosphor screen for 72 hours, and the density of the spots was measured and analyzed by means of array software (ScanAnalyze).

# Supplemental Experimental Procedures

### Isolation and Treatments of DCs and MDSCs

Splenic DCs were purified using CD11c MicroBeads (Miltenyi Biotec) in the presence of EDTA to disrupt DC-T cell complexes. Cells were 90-95% $CD11c^+$, >95% MHC $I\text{-}A^+$, >95% $B7\text{-}2^+$, <0.1% $CD3^+$, and appeared to consist of 90–95% $CD8^-$, 5–10% $CD8^+$, and 1–5% $B220^+PDCA^+$ (i.e., plasmacytoid DCs or pDCs) cells (Grohmann et al., 2002) (Figure S5B and data not shown). Although the presence of a small percentage of pDCs (previously demonstrated to activate the IDO1 signaling in response to TGF-β (Pallotta et al., 2011)) may raise the possibility that Arg1 and IDO1 pathways are occurring in distinct DC subsets, we demonstrated by immunofluorescence that cDCs do upregulate both Arg1 and IDO1 proteins following TGF-β stimulation (Figure S5A) and, by Real-Time PCR, that also purified pDCs can upregulate the gene expression of both amino acid catabolizing enzymes (Figure S5C). DC populations were further fractionated according to CD8 expression to obtain purified $CD8^-$ DCs by means of selective MicroBeads (Miltenyi Biotec). The $CD8^-$ fraction was 45% $CD4^+$ and typically contained <0.5% contaminating $CD8^+$ cells.

MDSCs were obtained from bone marrow cells, harvested and plated at $1 \times 10^6$ cells/ml in RPMI 1640 medium (Thermo Fisher Scientific) supplemented with 10% FCS, 10 ng/ml recombinant mouse (rm) GM-CSF (Peprotech), 10 ng/ml rmIL-4 (Peprotech) plus 30% v/v of tumor cell conditioned medium (TCCM) from B16F10 tumor cells, as previously described (Youn et al., 2008). Cultures were incubated at 37°C for five days. On day 3, fresh medium with cytokines and TCCM was replaced. Cells were collected on day 5 and analyzed by flow cytometry for CD11b and Gr1 expression. Recovered cells routinely resulted > 70 % co-expressing CD11b and Gr1.

Peripheral blood mononuclear cells (PBMCs) were cultured to produce human monocyte-derived DCs as previously described (Woltman et al., 2003). Briefly, PBMCs were isolated from a buffy coat obtained from healthy donors using Ficoll-Hypaque (GE Healthcare Life Science) density gradient centrifugation and were plated at density of $2 \times 10^6$ cells/ml in 6-well tissue culture dishes. After 2 hr at 37°C, non-adherent cells were removed by washing twice with cold PBS. The adherent fraction was cultured in RPMI 1640 medium (Thermo Fisher Scientific) supplemented with 10% FCS, 20 ng/ml recombinant human (rh) GM-CSF (Peprotech) and 20 ng/ml rhIL-4 (Peprotech). Cultures were incubated at 37°C for seven days. On day 4, fresh medium with cytokines at the same dosages was replaced.

For all in vitro studies, $CD11c^+$ or $CD8^-$ DCs were cultured at $1 \times 10^6$ cells per well in 24-well plates in Iscove's Modified Dulbecco's medium (IMDM, Thermo Fisher Scientific) or, in selected experiments, in

Dulbecco's Modified Eagle Medium (DMEM, Thermo Fisher Scientific), containing low or standard Arg levels (4, 40, or standard 400 μM) and completed by adding L-asparagine (120 μM) and L-lysine (790 μM). rmIL-4 and rmIFN-γ (Peprotech) were used to stimulate DCs at the final concentration of 10 ng/ml and 100 U/ml, respectively. Arg, Orn, and polyamines (putrescine, spermidine and spermine) were from Sigma-Aldrich. The Arg1 inhibitor nor-NOHA (Bachem) was used at a final concentration of 50 or 100 μM. DFMO (Sigma-Aldrich) was used at the final concentration of 1 mM. PP2 (an Src inhibitor), and PP3 (negative control for the Src inhibitor; both from Tocris Bioscience), were used at the final concentration of 5 μM. The TGF-β receptor signaling inhibitors SB-431542, LY-2109761, and LY2157299 were purchased from Cayman Chemical and used at the final concentration of 10 μM. In specific experiments, DCs were conditioned by co-culture for 24 hr with MDSCs (either such or pretreated for 1 hr with Nor-NOHA or DFMO using transwell cell culture inserts (Nunc).

### Real-Time RT-PCR and Western Blotting

Real-Time RT-PCR (for mouse *Ido1*, *Arg1*, *Ptpn6*, *Tgfb1*, and *Gapdh*) analyses were carried out as described (Pallotta et al., 2011), using primers listed in Table S2. Data were calculated as the ratio of gene to *Gapdh* expression by the relative quantification method (ΔΔCT; means ± SD of triplicate determination), and data are presented as normalized transcript expression in the samples relative to normalized transcript expression in control cultures (in which fold change = 1; dotted line). Anti-Src, and -pSrc (Tyr416), antibodies were from Cell Signaling Technology, whereas anti−β-tubulin was from Sigma-Aldrich.

### Determination of Arg1 and IDO1 Catalytic Activity

Arg1 activity was measured in cell lysates in terms of urea production, as described (Bronte et al., 2003). The urea concentration was determined by measuring absorbance at 430 nm by means of a spectrophotometer, and then normalized for the total protein content. IDO1 functional activity was measured in culture supernatants in terms of the ability to metabolize L-tryptophan to Kyn, whose concentrations were measured by high performance liquid chromatography in 24 hr−culture supernatants after the addition of 100 μM L-tryptophan for the final 8 hr (Fallarino et al., 2003; Grohmann et al., 2007).

### Meta-analysis of Dendritic Cell Gene Expression Data

*Microarray data collection and processing*. Gene expression data of DCs, obtained using Mouse Gene 1.0 ST and Mouse Genome 430 2.0 arrays, were downloaded from Gene Expression Omnibus

(http://www.ncbi.nlm.nih.gov/geo) and ArrayExpress (https://www.ebi.ac.uk/arrayexpress/). Accession numbers of samples used in this study are listed in Table S3. Microarray probe fluorescence signals of samples belonging to the same type of array were converted to expression values using the Robust Multiarray Average procedure (Irizarry et al., 2003) coded in the *affy* Bioconductor package. Briefly, fluorescence intensities were background-adjusted and normalized using quantile normalization, and expression values were calculated using median polish summarization and Entrez-based chip definition files for Mouse Gene 1.0 ST Array (mogene10stv1_Mm_ENTREZG version 15.0.0; 21225 custom probe sets) and for Mouse Genome 430 2.0 Array (Mouse4302_Mm_ENTREZG version 15.0.0; 17306 custom probe sets), respectively (Dai et al., 2005). All data analyses were performed in R version 2.14.2 using Bioconductor libraries and R statistical packages.

*Merging of Gene 1.0 ST and Mouse Genome 430 transcriptional data.* Transcriptional data of samples hybridized on Mouse Gene 1.0 ST arrays were merged with those obtained with Mouse Genome 430 2.0 arrays matching 16547 common Entrez gene IDs, i.e., the common identifier of custom probe sets in both data sets. A direct merging of raw fluorescence signals (i.e., of CEL files), although desirable for an optimal removal of batch effects, was unfeasible due to the different probe sequences synthesized on Mouse Gene 1.0 ST and Mouse Genome 430 arrays. Thus, batch effects were removed applying ComBat to the merged matrix. ComBat was used with default parameters with the exception of the adjustment variables that were imputed as a vector of array type labels (Johnson et al., 2007).

## Metabolomic Analyses

For metabolomic analysis, DCs (1 x $10^6$ cells/sample; in triplicate) were incubated in the presence or absence of Orn at 100 µM. After 4 and 16 hr, supernatants were collected to perform extraction of metabolites as described (D'Alessandro et al., 2014; Viticchie et al., 2015). Twenty µl of extract for each sample were injected into a system of ultraperformance liquid chromatography-high resolution mass spectrometry (UPLC-HRMS) (Ultimate 3000, Thermo) and running on a positive mode. Samples were loaded onto a ReproSil C18 column (2.0 mm × 150 mm, 2.5 µm — Dr. Maisch GmbH) and chromatographic separations were achieved at a temperature of 30 °C and flow rate of 0.2 ml/min. The UPLC system was coupled online with a mass spectrometer Q Exactive (Thermo) scanning in full MS mode (2 µscans) at 70,000 resolution. Calibration was performed before each analysis against positive ion mode calibration mixes (Piercenet, Thermo Fisher) to ensure sub ppm error of the intact mass. Metabolite assignments were performed using computer software (Maven), upon conversion of .raw files into .mzXML format through MassMatrix.

## Kinome Profiling Analyses

DCs were lysed in ice-cold Pepchip cell lysis buffer (20 mM Tris-HCl, pH 7.5, 150 mM NaCl, 1 mM $Na_2EDTA$, 1 mM EGTA, 1% Triton X-100, 2.5 mM sodium pyrophosphate, 1 mM $MgCl_2$, 1 mM µ-glycerophosphate, 1 mM $Na_3VO_4$, 1 mM NaF, 1 µg/ml leupeptin, 1 µg/ml aprotinin, 1 mM PMSF). Samples were sonicated four times for 5 s each time on ice and centrifuged at 7000 × *g* for 10 min at 4°C. Protein content in the clear supernatant was determined with a bicinchoninic acid protein assay kit (Pierce, Rockford, IL), using bovine serum albumin (BSA) as standard, and supernatants were stored at −80°C until peptide array analysis. For peptide array analysis, we employed the Pepchip kinomics array, featuring 960 different human-only kinase substrate peptides in addition to 70 positive and negative controls, each spotted in triplicate. Cell lysates were cleared by centrifugation and peptide array incubation mix was produced by adding 10 µl of activation mix (50% glycerol, 50 µM ATP, 0.05% v/v Brij-35, and 0.25 mg/ml BSA) and 2 µl [$\gamma$-$^{33}$P] ATP (approx. 1000 kBq (Amersham AH9968). Next, the peptide array mix was added onto the chip, which was kept at 37°C in a humidified stove for 90 min. Subsequently, the peptide array was washed twice with Tris-buffered saline with Tween 20, twice in 2 M NaCl, and twice in demineralised $H_2O$ and then air-dried. The chips were exposed to a phosphor screen for 72 hours, and the density of the spots was measured and analyzed by means of array software (ScanAnalyze). Using grid tools, spot density and individual background were corrected and spot intensities and background intensities were analyzed. Data were exported to an excel sheet (Table S4) for further analysis.

# Supplementary Text

## Role of TGF-βR Subunits in Arg1-Mediated IDO1 Signaling

Activation of the TGF-β receptor type II subunit (TGF-βRII) by TGF-β binding is known to be absolutely required for activation of the TGF-βRI kinase and subsequent triggering of the TGF-βR signaling, either Smad-dependent or Smad-independent, including that mediated by PI3K (Gorelik and Flavell, 2002; Pickup et al., 2013; Tu et al., 2014). We previously demonstrated that the mechanisms involved in the activation of IDO1 signaling by TGF-β are rather complex, being IDO1 phosphorylation (which happens early) Smad-independent but PI3K-dependent, whereas the later induction of SHP phosphatases is contingent on both Smad and PI3K (Pallotta et al., 2011). In order to evaluate whether autocrine/paracrine TGF-β could play a role in the effects of ornithine (Orn) in DCs, wild-type (WT) DCs were incubated with the Arg metabolite for different times after a 1-hr pretreatment with an inhibitor of TGF-β receptor signaling, namely, SB-431542 (selective for TGF-βRI or ALK5), LY2109761 (inhibiting both TGF-βRI and TGF-βRII), or LY2157299/galunisertib (targeting TGF-βRI) (Figure 3D). DCs purified from transgenic $CD11^{cdnR}$ mice (expressing a truncated form of TGF-βRII in $CD11c^{+}$ cells) (Laouar et al., 2005) were also assayed (Figure 3E). Our findings showed that inhibition of TGF-βRI (as provided by all tested TGF-βR inhibitors) is apparently more effective than functional inactivation of TGF-βRII alone (as occurs in $CD11^{cdnR}$ DCs). Although difficult to reconcile with the widely accepted view of TGF-βR signaling, our data may be explained by data provided by Ishigame et al. in a *Listeria* infection model, which suggested that $CD11^{cdnR}$ mice perhaps still express a functional TGF-βRII that can induce some level of TGF-β signaling (Ishigame et al., 2013). Moreover, Xavier et al reported that TGF-βRI may trigger TGF-βR signaling (both Smad and PI3K-dependent) independently from the other subunit (Xavier et al., 2009). Whatever the true mechanism/s will be, our current data do indicate that the TGF-βR signaling is involved in the *Ido1* upregulating effects of Orn in DCs.

## REFERENCES


Blasius, A.L., Giurisato, E., Celia, M., Schreiber, R.D., Shaw, A.S., and Colonna, M. (2006). Bone marrow stromal cell antigen 2 is a specific marker of type I IFN-producing cells in the naive mouse, but a promiscuous cell surface antigen following IFN stimulation. Journal of Immunology *177*, 3260-3265.

D'Alessandro, A., Amelio, I., Berkers, C.R., Antonov, A., Vousden, K.H., Melino, G., and Zolla, L. (2014). Metabolic effect of TAp63alpha: enhanced glycolysis and pentose phosphate pathway, resulting in increased antioxidant defense. Oncotarget *5*, 7722-7733.

Dai, M., Wang, P., Boyd, A.D., Kostov, G., Athey, B., Jones, E.G., Bunney, W.E., Myers, R.M., Speed, T.P., Akil, H., *et al.* (2005). Evolving gene/transcript definitions significantly alter the interpretation of GeneChip data. Nucleic acids research *33*, e175.

Gorelik, L., and Flavell, R.A. (2002). Transforming growth factor-beta in T-cell biology. Nature Reviews Immunology *2*, 46-53.

Grohmann, U., Orabona, C., Fallarino, F., Vacca, C., Calcinaro, F., Falorni, A., Candeloro, P., Belladonna, M.L., Bianchi, R., Fioretti, M.C., *et al.* (2002). CTLA-4-Ig regulates tryptophan catabolism in vivo. Nat Immunol *3*, 1097-1101.

Irizarry, R.A., Hobbs, B., Collin, F., Beazer-Barclay, Y.D., Antonellis, K.J., Scherf, U., and Speed, T.P. (2003). Exploration, normalization, and summaries of high density oligonucleotide array probe level data. Biostatistics *4*, 249-264.

Ishigame, H., Mosaheb, M.M., Sanjabi, S., and Flavell, R.A. (2013). Truncated Form of TGF-beta RII, But Not Its Absence, Induces Memory CD8(+) T Cell Expansion and Lymphoproliferative Disorder in Mice. Journal of Immunology *190*, 6340-6350.

Johnson, W.E., Li, C., and Rabinovic, A. (2007). Adjusting batch effects in microarray expression data using empirical Bayes methods. Biostatistics *8*, 118-127.

Laouar, Y., Sutterwala, F.S., Gorelik, L., and Flavell, R.A. (2005). Transforming growth factor-beta controls T helper type 1 cell development through regulation of natural killer cell interferon-gamma. Nat Immunol *6*, 600-607.

Pallotta, M.T., Orabona, C., Volpi, C., Vacca, C., Belladonna, M.L., Bianchi, R., Servillo, G., Brunacci, C., Calvitti, M., Bicciato, S., *et al.* (2011). Indoleamine 2,3-dioxygenase is a signaling protein in long-term tolerance by dendritic cells. Nat Immunol *12*, 870-878.

Pickup, M., Novitskiy, S., and Moses, H.L. (2013). The roles of TGFbeta in the tumour microenvironment. Nature reviews Cancer *13*, 788-799.

Tu, E., Chia, P.Z., and Chen, W. (2014). TGFbeta in T cell biology and tumor immunity: Angel or devil? Cytokine Growth Factor Rev *25*, 423-435.

Viticchie, G., Agostini, M., Lena, A.M., Mancini, M., Zhou, H., Zolla, L., Dinsdale, D., Saintigny, G., Melino, G., and Candi, E. (2015). p63 supports aerobic respiration through hexokinase II. Proc Natl Acad Sci U S A *112*, 11577-11582.

Woltman, A.M., van der Kooij, S.W., Coffer, P.J., Offringa, R., Daha, M.R., and van Kooten, C. (2003). Rapamycin specifically interferes with GM-CSF signaling in human dendritic cells, leading to apoptosis via increased p27KIP1 expression. Blood *101*, 1439-1445.

Xavier, S., Niranjan, T., Krick, S., Zhang, T.R., Ju, W.J., Shaw, A.S., Schiffer, M., and Bottinger, E.P. (2009). T beta RI Independently Activates Smad- and CD2AP-Dependent Pathways in Podocytes. J Am Soc Nephrol *20*, 2127-2137.

Youn, J.I., Nagaraj, S., Collazo, M., and Gabrilovich, D.I. (2008). Subsets of myeloid-derived suppressor cells in tumor-bearing mice. J Immunol *181*, 5791-5802.